Journal Pre-proofs

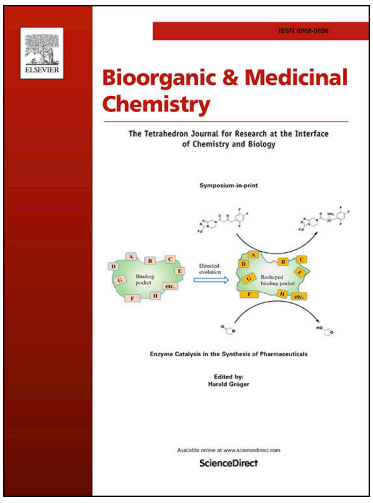

New modification strategy of matrine as Hsp90 inhibitors based on its specific L conformation for cancer treatment

Yiming Xu, Dewang Jing, Dong Zhao, Yongji Wu, Lu Xing, Haroon ur Rashid, Haodong Wang, Lisheng Wang, Huiling Cao

PII: S0968-0896(19)31415-4
DOI: https://doi.org/10.1016/j.bmc.2020.115305
Reference: BMC 115305

To appear in: *Bioorganic & Medicinal Chemistry*

Received Date: 22 August 2019
Revised Date: 22 December 2019
Accepted Date: 2 January 2020

Please cite this article as: Y. Xu, D. Jing, D. Zhao, Y. Wu, L. Xing, H. ur Rashid, H. Wang, L. Wang, H. Cao, New modification strategy of matrine as Hsp90 inhibitors based on its specific L conformation for cancer treatment, *Bioorganic & Medicinal Chemistry* (2020), doi: https://doi.org/10.1016/j.bmc.2020.115305

New modification strategy of matrine as Hsp90 inhibitors based on its specific L conformation for cancer treatment

Yiming Xu[a,c,†], Dewang Jing[c,†], Dong Zhao[b], Yongji Wu[d], Lu Xing[b], Haroon ur Rashid[c,e], Haodong Wang[c], Lisheng Wang[a,*] and Huiling Cao[b,*]

[a] *Medicinal College, Guangxi University, Nanning 530004, China;*

[b] *Shaanxi Key Laboratory of Ischemic Cardiovascular Disease, Institute of Basic Translational Medicine, Xi'an Medical University, Xi'an 710021, China;*

[c] *School of Chemistry and Chemical Engineering, Guangxi University, Nanning 530004, China;*

[d] *College of Veterinary Medicine, Northwest A&F University, Yangling 712100, China;*

[e] *Department of Chemistry, Sarhad University of Science & Information Technology, Peshawar, Khyber Pakhtunkhwa 25120, Pakistan;*

[*] *Correspondence: lswang@gxu.edu.cn; caohuiling_jzs@xiyi.edu.cn;*

[†] *These authors contributed equally to this work;*

Abstract

The similarity of spatial structure between radicicol and matrine urged us to perform conformation modification of matrine, followed by L-shaped matrine derivatives, **6**, **12**, **21a-h** and **22a-h** were originally designed, synthesized and evaluated for $Hsp90^N$ inhibitors as anticancer agents. TSA (Thermal Shift Assay) results indicated that **21e**, **22a-c** and **22e-g** exhibited strong binding force against $Hsp90^N$ with $|\Delta Tm| > 3$, meanwhile, MTT assay also revealed these compounds displayed potent anticancer activity with IC_{50} values below 25 μM against HepG2, HeLa and MDA-MB-231 cells lines. Then, compound **22g** with a high $\Delta Tm = 10.92$ was chosen as a representative to perform further mechanism study. It can induce cell apoptosis, arrest the cell cycle at the S phase and decrease the expression level of Hsp90 in Hela cell. These results originally provided targeted modification strategy for matrine derivatives to serve as Hsp90 inhibitors for cancer therapy.

Keywords: L-shaped matrine derivatives; Radicicol; Thermal Shift Assay; Anticancer activity; Mechanism of action;

Introduction

Matrine (**Fig. 2d**), a quinolizidine natural product extracted from *Sophora flavescens* (Kushen) [1-4], was approved by Chinese FDA in 1995 for cancer treatment. Currently, matrine has been widely used to adjuvant treatment of liver cancer, lung carcinoma and gastric cancer with low side effects for many years in China [5-6]. Although large-scale application of matrine with reference to its use for the treatment of cancer was confirmed [7-11], its activity is moderate, which might be caused by its speculated features such as broad binding sites but low specificity. Thus, enhancing the sensibility and specificity against anticancer targets of matrine attracted our attention. On the other hand, matrine possess many advantages such as high solubility, good safety profiles and a special chemical scaffold, suggesting that it is an ideal lead compound for further modifications and optimizations to treat cancer.

Recently, our group also conducted a comprehensive literature review (**Fig. 1**) on modification strategy of matrine [12]. As illustrated in **Fig. 1**, lots of matrine derivatives have been synthesized through various modifications on different positions of matrine. However, up to now, research on targeted design for matrine derivatives is still not be involved which caused blindness for their development. Different from traditional cytotoxic chemotherapy, targeted therapy has many advantages, such as high specificity, good efficacy and low toxicity. Inspired by above suggestions, targeted design for matrine might be an effective strategy to discover anticancer candidates of matrine derivatives.

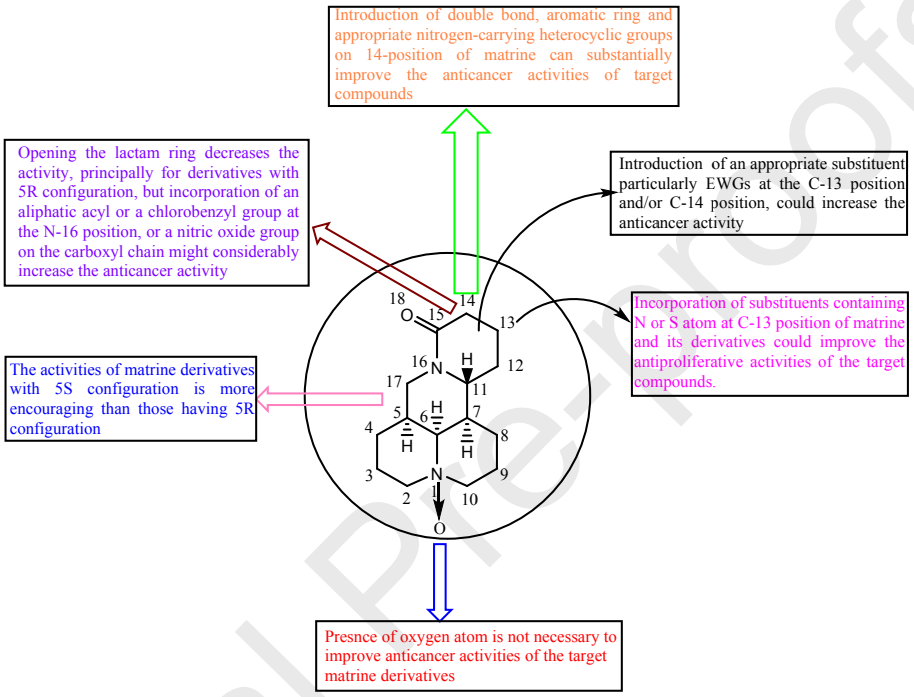

Fig. 1 Modification strategy of matrine and SAR study reported in literature review [12]

Interestingly, the specific L-shaped conformation of matrine is similar with radicicol (**Fig. 2**). Besides, radicicol serves as a $Hsp90^N$ inhibitor and its molecular mechanism has been thoroughly studied, which provided possibility for structural modification of matrine derivatives to target $Hsp90^N$ based on radicicol conformation analysis. Moreover, the overexpressed characteristics in tumor cells and the prospect of stalling a number of oncogenes by inhibiting a single protein have made Hsp90 an attractive target for cancer therapy [13-15]. Thus, by targeted design and inhibiting the activity of Hsp90, it might be an effective strategy for matrine modifications to treat cancer.

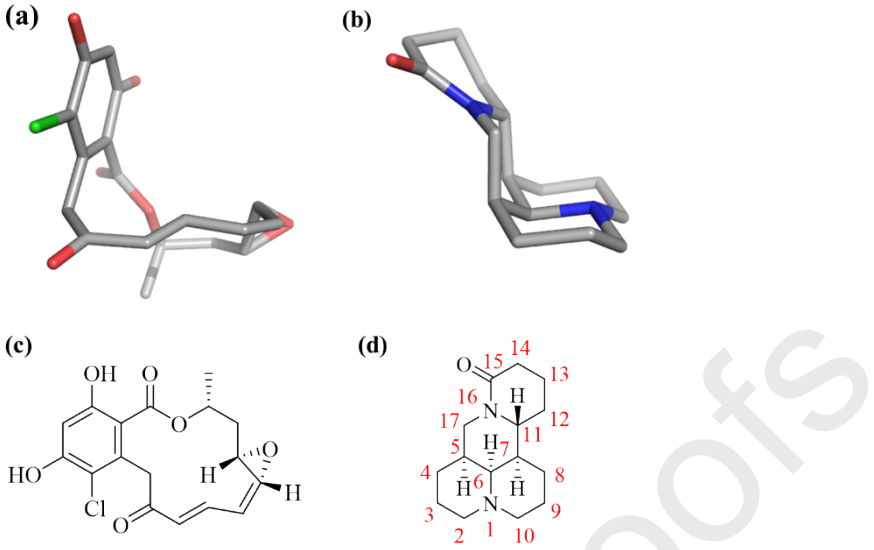

Fig. 2 L-shaped 3D conformation of radicicol **(a)** and matrine **(b)**; Molecular structures of radicicol **(c)** and matrine **(d)**.

Drug design

Radicicol, as the Hsp90^{N} inhibitor, its mechanism involves a competition with ATP at N-terminal ATP-binding pocket of Hsp90, resulting in the inactivation of protein [16-17]. The co-crystal structures [18] revealed that the binding mode of planar moiety in radicicol with N-terminal ATP-binding pocket is similar to that of adenine moiety in ATP, through which it can directly form hydrogen bond with residues or via a water-mediated network of hydrogen bonds (**Fig. 3a, c**) and then "occupy" the adenine aisle. Another moiety of the radicicol mainly participated in the specific L-conformation formation. We speculated that the specific conformation can not only "capture" the planar moiety to the suitable site at the aisle without penetrating deep into it, but also "close" the ATP entrance (**Fig. 3b, d**).

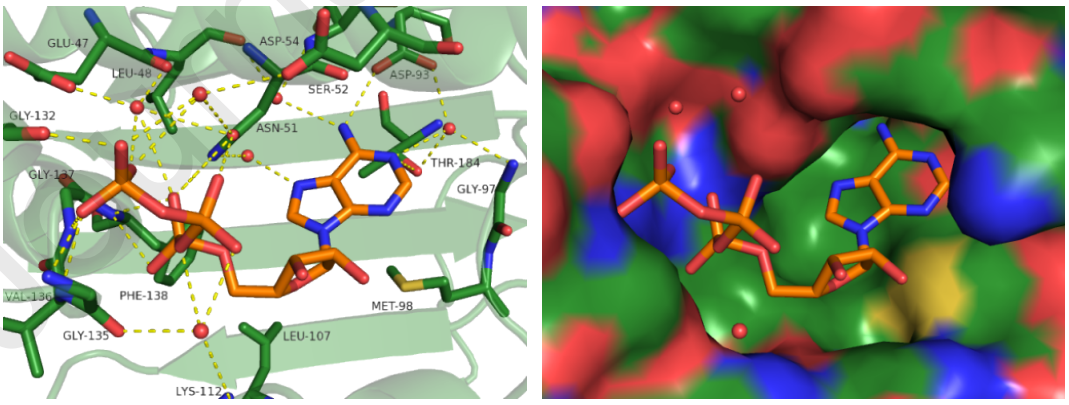

(a) **(b)**

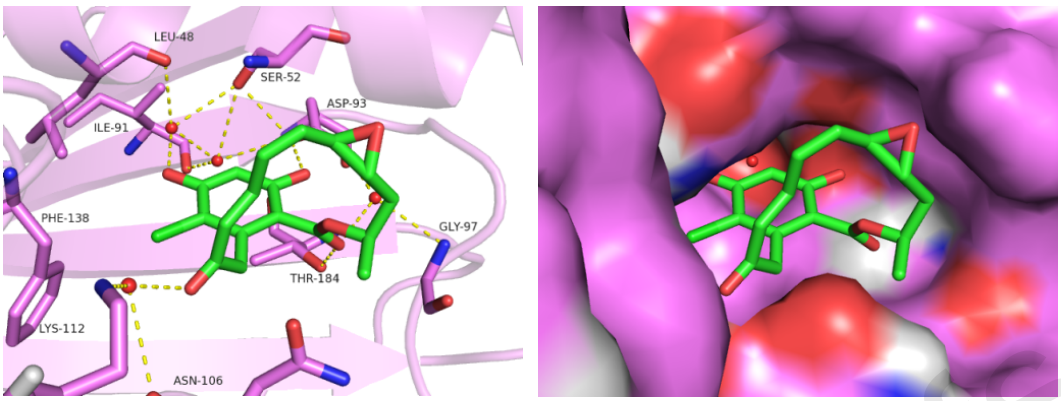

(c) **(d)**

Fig. 3 (a) Binding mode of ATP with Hsp90 and **(b)** Modeling of ATP represented as a surface [PDB code: 3T0Z]; **(c)** Binding mode of radicicol and **(d)** Modeling of radicicol represented as a surface [PDB code: 4EGK].

The lack of planar structure with hydrophilic and halogen groups is the main difference of scaffolds between matrine and radicicol (**Fig. 2c, d**), which act as a targeted warhead to N-terminal ATP-binding pocket. Additionally, the spatial L conformation of matrine similar with radicicol (**Fig. 2a, b**) could block the cavity to prevent ATP entrance. Thus, based on radicicol structure and its mechanism, planar structure with hydrophilic group and halogen group was introduced into matrine to enhance the targeting effect towards Hsp90, meanwhile, the hybridization should keep derivatives in L conformation.

In present study, two modification strategies were adopted. First, we hypothesized that the variation in size of the conformation might influence the activity. Thus, enlargement and contraction were performed via D-ring modifications of matrine. Second, planar structure with substituents was built on matrine scaffold (**Scheme 1**.).

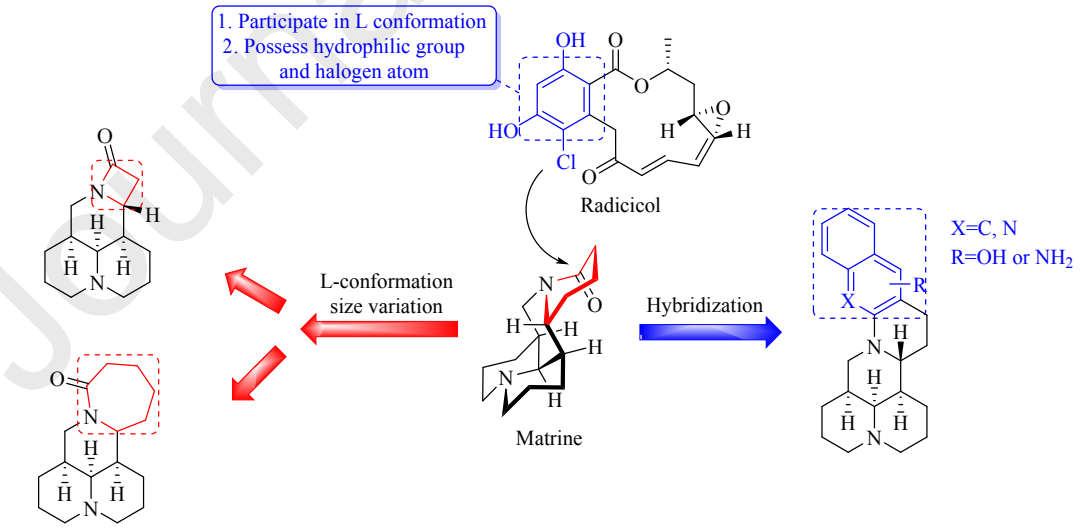

Scheme 1. The modification strategy for L-shaped matrine derivatives based on radicicol.

Chemistry

The synthetic route of lactam D ring contraction for the synthesis of derivative **6** is depicted in **Scheme 1**. Matrine was first treated with n-butylithium to gain carbanion intermediate, followed by its substitution with **2**, and oxidation via IBX to gain **3**. Then **3** was subjected to elimination, using K_2CO_3 in toluene under reflux to produce sophocarpine **4** [19]. β-amino acid **5** was obtained via the cleavage of lactam and alkenyl bond in **4** by its treatment with $KMnO_4$ in 10% H_2SO_4 aqueous. Finally, after screening, Mukaiyama's reagent [20] was used to activate the carboxyl group for the formation of β-lactam of **6**.

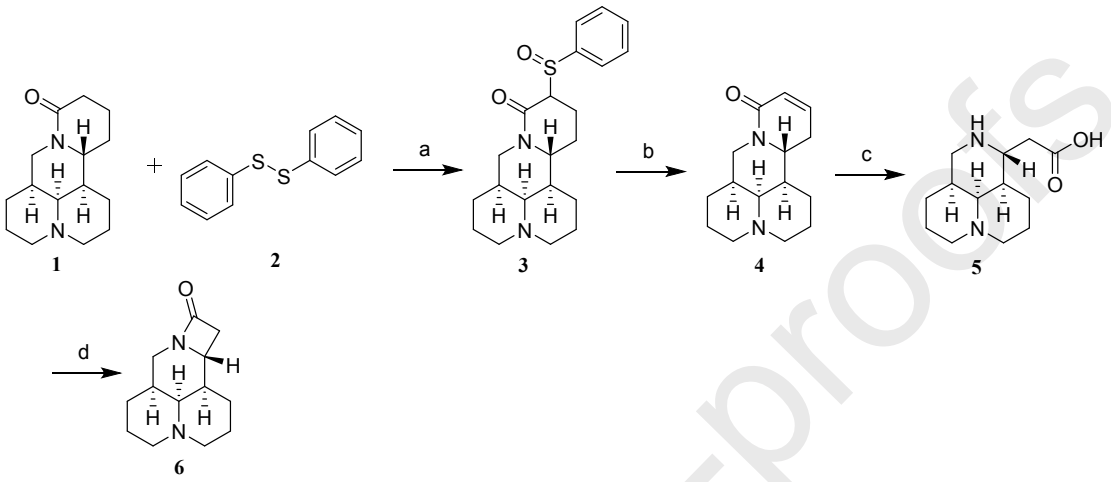

Scheme 2. Reagents and conditions: (a) (i) diisopropylamine, n-butylithium, matrine, THF, -78 °C to 25 °C, 1h; diphenyl disulfide, 2h; (ii) IBX, HCl aqueous, 50 °C~70 °C, 3h; (b) K_2CO_3, toluene, reflux, 1.5 h; (c) 10% H_2SO_4 aqueous, $KMnO_4$, reflux, 2 h; (d) 2-chloro-1-methylpyridinium iodide, Et_3N, CH_2Cl_2/1, 4-dioxane, rt, overnight. IBX = 2-iodoxybenzoic acid.

The synthetic route of **12** is shown in **Scheme 3**. Acid **7** was prepared by hydrolysis of matrine in aqueous KOH under reflux, followed by acidification with HCl. Then, fluorenylmethoxy carbonyl, as a protecting group, was introduced on nitrogen atom to produce **8**. Thionyl chloride was added to dichloromethane solution of **8** to form corresponding acyl chloride followed by treatment with $TMSCHN_2$, which facilitated the diazotization smoothly in relatively high yield and purity. With silver oxide as a catalyst, α-diazoketone **9** was transformed to acid **10** through Wolff rearrangement [21]. Deprotection of **10** was completed in 10 % NaOH aqueous to obtain **11**. Finally, HATU was verified as an efficient polypeptide condensation reagent for the synthesis of target **12** working at low concentrations of **11** in order to suppress possible intermolecular side reactions [22].

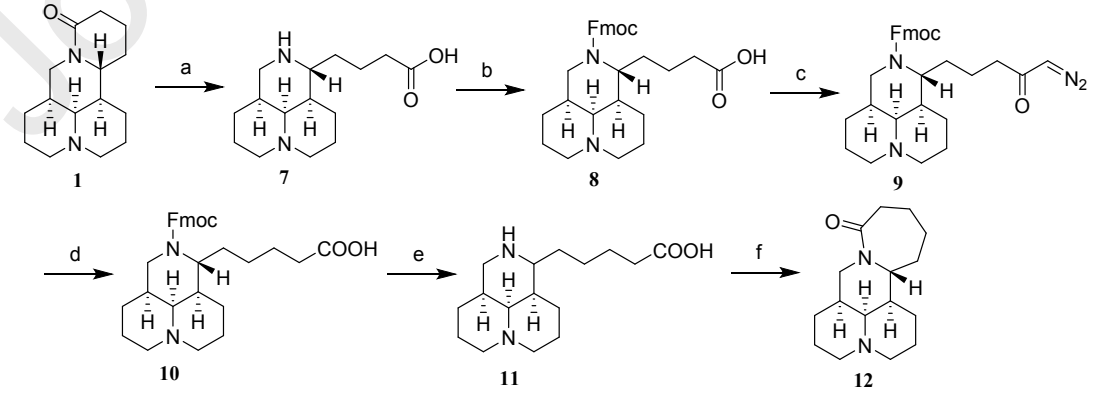

Scheme 3. Reagents and conditions: (a) 5 N NaOH aqueous, reflux, overnight; HCl, pH to 5~6; (b) Na_2CO_3, Fmoc-Cl,

1, 4-dioxane/H_2O, rt, 6~8 h; (c) (i) $SOCl_2$, CH_2Cl_2, reflux, 1~2 h, N_2 protection; (ii) $TMSCHN_2$, CH_2Cl_2, -15 °C~-20 °C, 1~2 h; (d) Ag_2O, Na_2CO_3, $NaHSO_3$, 1, 4-dioxane/H_2O, 50 °C~60 °C, 2~3 h; HCl, pH to 5~6; (e) 10 % NaOH aqueous, rt, 1~2h; HCl, pH to 5~6; (f) HATU, DIPEA, THF/DCM, rt, overnight.

Aiming at the synthesis of quinolionmatrinic derivatives, a retrosynthetic analysis is first given in **Scheme 4**. The target compound **13** could be disconnected directly at 14-position to produce synthon **14**. It is notable that compound **13** can be transformed to **16** by functional group addition strategy. Then the double bond fragment of **16** could be formed by a base-mediated cyclization of an amidine **17** (Friedländer type cyclization), bearing an aromatic ester or a nitrile (R) functional group. Considering the importance of amino and hydroxyl groups as hydrogen bond donor in medicinal field, compound **17** was chosen as an intermediate synthon. Finally, compound **17** can be disconnected to produce starting material **1** and **18**.

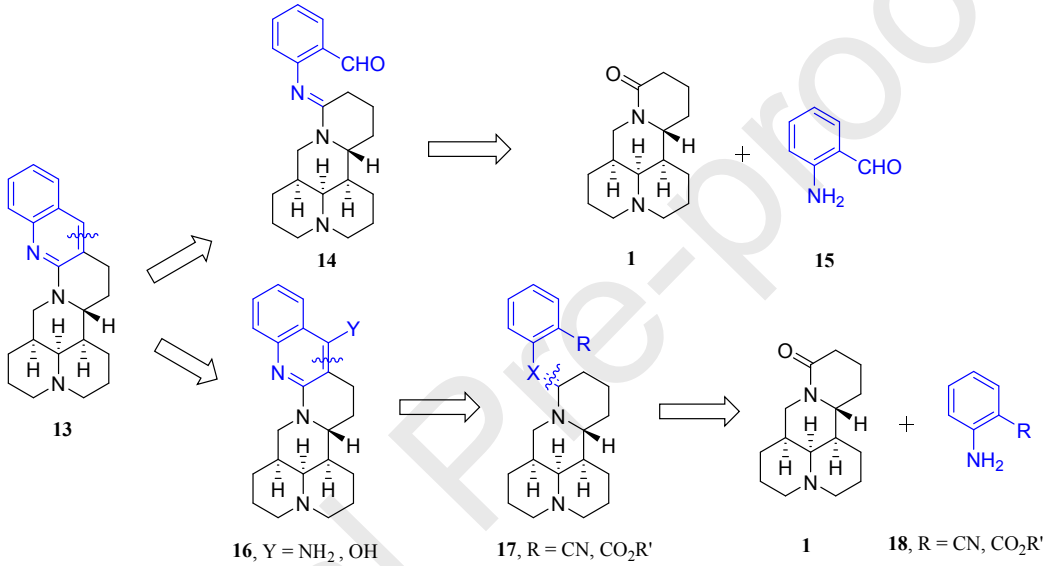

Scheme 4. Retrosynthetic analysis of ring-constrained quinolinomatrinic derivatives.

As depicted in **Scheme 5**, matrine was treated with $POCl_3$ to afford the corresponding α-choroiminiums, which react efficiently with nucleophiles, including amines. However, the formation, as an intermediate, of a highly strained bridgehead iminium species remains challenging [23]. Suitable reaction conditions were gained after screening ($POCl_3$ 2 eq., CH_2Cl_2, reflux for 2.5 h) in order to obtain a useful α-chloroenamine intermediate **19**. Considering the role of Schiff base in pharmaceutical activities, such as antibacterial [24-25], antihypertensive [26], anti-inflammatory [27] and anticancer [28-30], a series of aromatic amine was first reacted with matrine to yield the intermediate products **21a-h**. Subsequently, products **20a-h** were synthesized using anilines bearing cyan derivatives **18a-h**. The crystal data and refinement details of **21g** (CCDC 1819315) revealed the newly synthesized **21a-h** have E-configuration (**Fig. 4**). Then, Lithium diisopropylamide (LDA) was chosen as a base to mediate the cyclization of **20a-h** to produce the corresponding products **22a-h**.

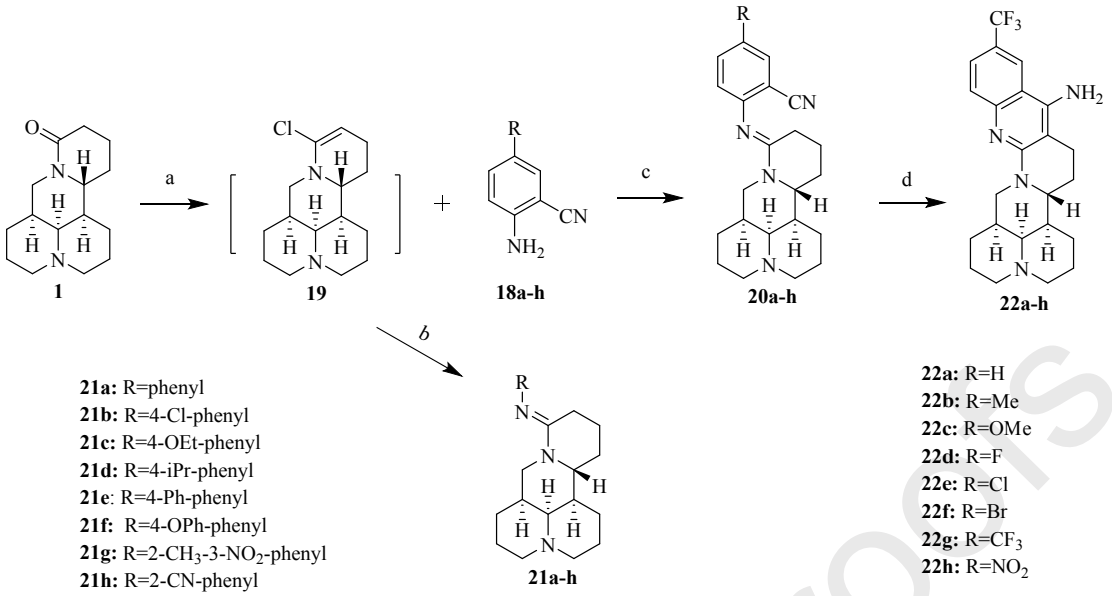

Scheme 5. Reagents and conditions: (a) $POCl_3$, DCM, 60 °C, 2~3 h; (b) aniline, DCM, reflux, 12 h; NaOH aqueous, pH to 8~9; (c) DCM, reflux, 12 h; NaOH aqueous, pH to 8~9; (d) LDA, anhydrous THF, 0 °C;

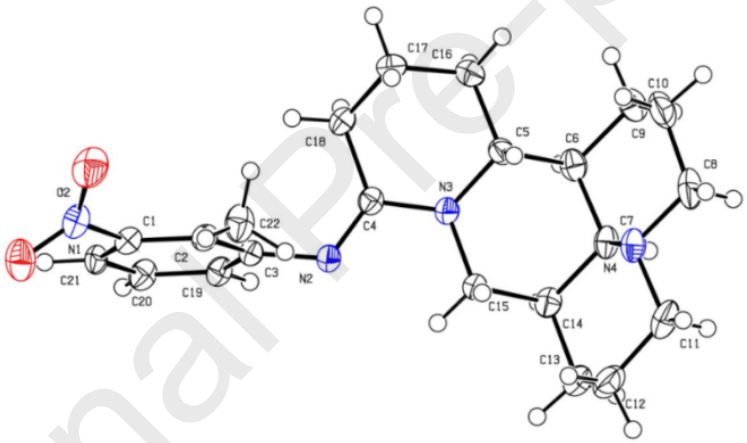

Fig. 4 Crystal structure of compound **21g** represented as ORTEP diagrams.

Thermal Shift Assay

Table 1. ΔTm (°C) values of matrine and its derivatives binding with $Hsp90^N$ measured by Thermal Shift Assay.

Ligand	ΔTm Mean (°C)	SD (n=8)
6	0.44	0.28
12	NT	NT
21a	-0.57	0.32
21b	NS	NS
21c	0	0.30
21d	-1.24	0.40
21e	-4.91	0.39
21f	-1.30	0.32

21g	-1.06	0.32
21h	-1.44	0.30
22a	-3.12	0.40
22b	-4.27	0.40
22c	-5.48	0.36
22d	-2.30	0.42
22e	-6.58	0.28
22f	-7.58	0.36
22g	10.92	0.60
22h	-0.24	0.28
Matrine	0.04	0.39
Radicicol	21.32	0.29

NT means not tested; NS means no fluorescence signal.

TSA (Thermal Shift Assay) is a method for detecting thermal stability of proteins, which quantitative real-time PCR is used to measure the melting curves of proteins with or without ligands and calculate Tm and ΔTm [31-33]. The larger | ΔTm | means stronger binding force between $Hsp90^N$ and ligand, whose | ΔTm | > 3 was usually considered as a ligand. TSA results indicated the Tm of $Hsp90^N$ was 47.63 ± 0.35 °C (**Fig. 5a**)**.** After $Hsp90^N$ binding with matrine and its derivatives, the Tm of all the complexs shifted to different degrees. Thereinto, the thermal shift of matrine, **6**, **21c** and **22g** binding with $Hsp90^N$ performed positive deviation with ΔTm＞0, indicating improvement in the $Hsp90^N$ thermal stability. While other compounds reduced the thermal stability of protein with ΔTm＜0 (**Table 1**).

On the other hand, there existed nine ligands made the Tm shift of $Hsp90^N$ more than 3 °C, among which **22a**, **22b** and **21e** possess | ΔTm | 3-5 (orange); **22c**, **22e** and **22f** possess | △Tm | 5-8 (green); importantly, **22g** possess | ΔTm | > 10 (red) (**Fig. 5c**). Meanwhile, the radicicol possess | ΔTm | > 20 (**Fig. 5d**). Moreover, matrine possess weak binding force with Hsp90 (**Fig. 5b**). The results preliminary illustrated the nine ligands exhibited strong binding force and targeted to $Hsp90^N$. It was originally confirmed that Hsp90 can serve as one directly target for matrine derivatives, providing theoretical basis for structural optimizations and exploring anticancer pathways of matrine.

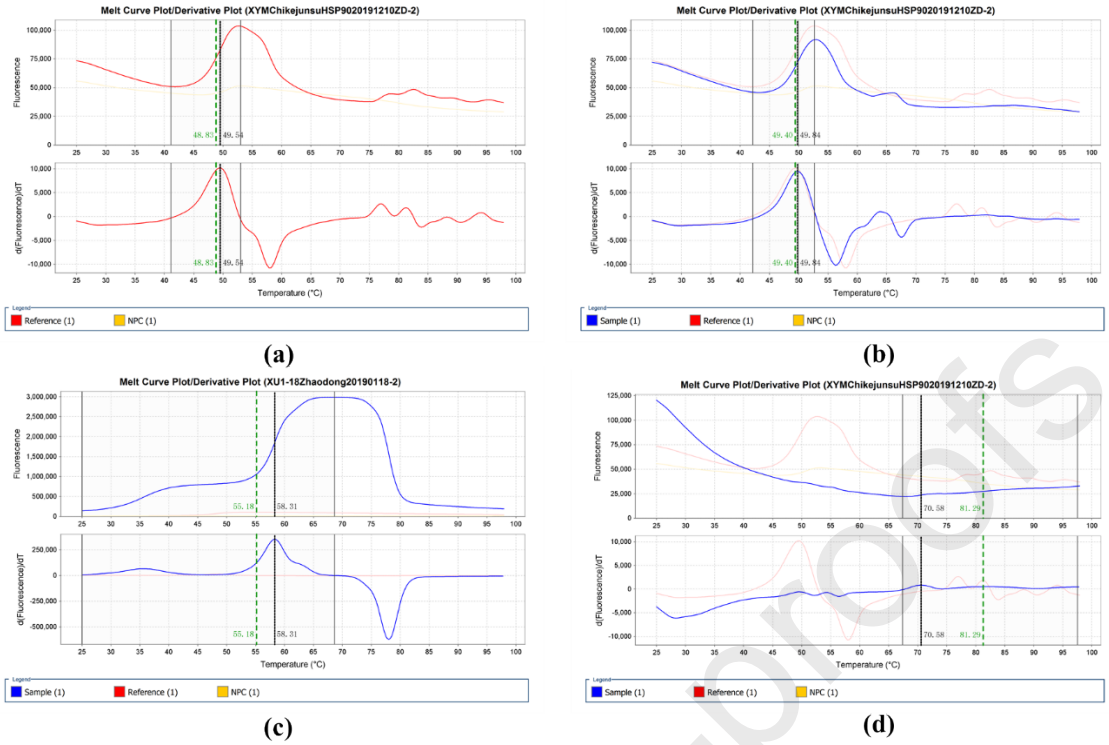

Fig. 5 Melting curves of the $Hsp90^N$ **(a)**, matrine binding with $Hsp90^N$ **(b)**, 22g binding with $Hsp90^N$ **(c)** and radicicol binding with $Hsp90^N$ **(d)**.

Anticancer activity *in vitro*

Table 2. IC_{50} values of compounds **6**, **12**, **21a-h** and **22a-h** against three cancer cells.

Entry	R	IC_{50} (μM)		
		HeLa	HepG2	MDA-MB-231
6		>100	>100	>100
12		>100	>100	>100
21a	H	>100	>100	>100
21b	4-Cl	>100	>100	73.4 ± 8.3
21c	4-OEt	>100	97.5 ± 2.6	>100
21d	4-iPr	93.3 ± 1.5	96.6 ± 4.3	77.5 ± 3.7
21e	4-Ph	23.7 ± 1.3	11.0 ± 0.5	24.6 ± 2.1
21f	4-OPh	33.7 ± 2.5	51.3 ± 4.5	55.2 ± 5.4
21g	$2\text{-}CH_3\text{-}3\text{-}NO_2$	>100	86.1 ± 8.9	>100
21h	2-CN	>100	>100	>100
22a	H	23.3 ± 1.4	14.3 ± 2.1	22.2 ± 1.8
22b	Me	13.4 ± 0.5	9.2 ± 1.2	16.9 ± 1.5
22c	OMe	18.0 ± 1.2	10.9 ± 2.9	21.2 ± 4.2
22d	F	18.8 ± 3.3	13.1 ± 1.9	37.3 ± 2.5
22e	Cl	8.9 ± 1.2	6.4 ± 0.3	14.3 ± 0.8
22f	Br	6.9 ± 0.8	9.7 ± 2.1	9.7 ± 1.5
22g	CF_3	19.6 ± 0.4	16.1 ± 3.2	22.1 ± 1.2

22h	NO_2	69.2 ± 4.6	35.1 ± 1.9	24.4 ± 3.4
Matrine		4332 ± 423	4509 ± 224	5372 ± 327
Cisplatin		19.2 ± 2.1	8.4 ± 3.4	48.9 ± 3.1

[a] IC_{50}: a concentration required to inhibit tumor cell proliferation by 50%. Data are expressed as the mean IC_{50} from the dose-response curves of at least three independent experiments.

Keeping in view the importance of Hsp90 as an attractive target for cancer therapy, the anticancer activity of all the target compounds against HepG2, HeLa and MDA-MB-231 cell lines was evaluated by MTT assay using cisplatin as positive drug control. Among the arylimidomatrinic derivatives **21a-h**, compounds **21e** exhibited potent activity against three cell lines as compared to matrine. While among quinolinomatrinic derivatives **22a-h**, compounds **22a-g** exhibited good activity with their IC_{50} below 25 μM against HepG2, HeLa and MDA-MB-231 cell lines. Notably, these compounds also showed strong binding force with $Hsp90^N$ (**Table 1**). These results also indicated the possibility of matrine modifications to target $Hsp90^N$ leading to potent activity for cancer treatment.

Structure-activity relationship (SAR) analysis of matrine derivatives was also performed. The TSA and MTT results of compounds **6**, **12** indicated the L-conformation change was made less effective via ring size variation. Among intermediate arylimidomatrinic derivatives, only **21e** showed potent anticancer activity and strong binding force with $Hsp90^N$, which indicated that the introduction of biphenyl could take an effective function. We speculated that the hydrophobic effect and extensibility of the molecular structure might be factors that affected the binding mode and biological activity. Structure-activity relationship (SAR) analysis was then focused on the quinolinomatrinic derivatives **22a-h**. Interestingly, all the compounds exhibited potent anticancer activities. Particularly, the IC_{50} values of compounds **22a-g** were below 25 μM. The general increase in activity and binding force with $Hsp90^N$ might be associated with the hydrophobic effect and building of L-conformation with the participation of quinoline ring. Besides, the R substituents could work on the activity and TSA results. Compounds **22b**, **22c** (R= electron-donating groups) and **22e**, **22f** (R=electron-withdrawing groups) all showed better MTT and TSA results than **22a**, which indicated inoperative electronic effects caused by the R substituents. We deduced that the R substituents also participated in L-conformation or exhibited hydrophobic effect and hydrogen bond interaction to react with $Hsp90^N$. In order to better understand the binding mode and mechanism of action of the synthesized derivatives, **22g** having the strongest binding force with $Hsp90^N$ and potent anticancer activity was chosen for further study.

Docking

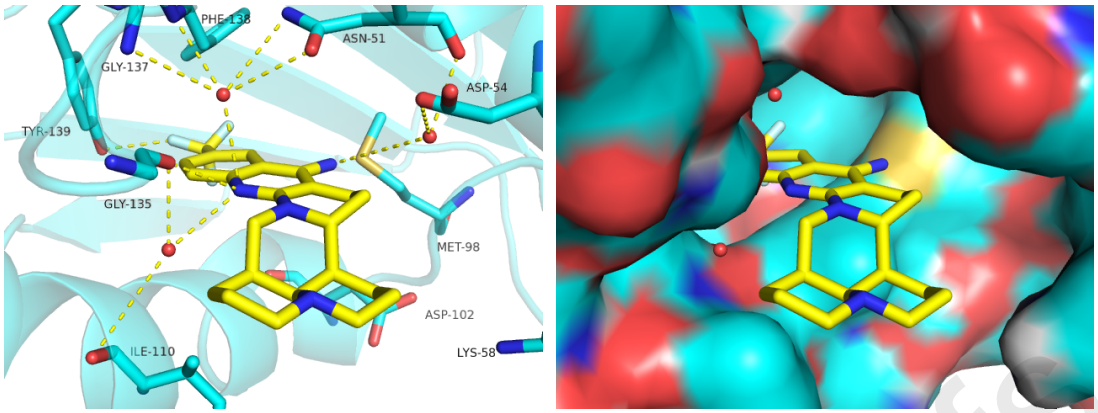

(a) **(b)**

Fig. 6 (a) Binding mode of compound **22g** with Hsp90 and **(b)** Modeling represented as surface. [PDB code: 1UYM]

The docking results of compound **22g** with Hsp90^{N} were depicted in **Fig. 6**. It's obvious that the quinoline ring moiety of **22g** could insert into the active cavity and its tert-nitrogen atom could form a water-mediated network of hydrogen bonds with PHE-138, ASN-51, GLY-137, GLY-135 and ILE-110. Similarly, the amino group on the quinoline ring, as a hydrogen donor, also interacted with ASN-51 and ASP-54 via water molecule. In regard to trifluoromethyl substituent, it not only can exhibit hydrophobic effect, but also form hydrogen bond with TYR-139 (**Fig. 6a**). More importantly, the planar quinoline ring and trifluoromethyl substituent participated in the L-conformation formation with matrine structure, which was analogous to radicicol. The specific conformation could enable the planar moiety to "occupy" the aisle and "close" the ATP entrance by matrine moiety (**Fig. 6b**). The binding mode originally provides theoretical basis for designing novel matrine derivatives as Hsp90 inhibitors.

Cell cycle analysis

We further analyzed the impact of compound **22g** upon cell cycle distribution. After treatment for 48h, compound **22g** induced obvious S phase arrest in HeLa cells (**Fig. 7**). In control group, the cells in S phase represented 17.24%, in the presence of 5, 10 and 20 μM of compound **22g**, it increased to 21.64%, 26.67%, and 40.12%, respectively, in a concentration dependent manner. Accordingly, there was a marked decrease in the percentage of cells in the G0/G1 phase after compound **22g** treatment. These results revealed that compound **22g** arrested the HeLa cell cycle at the S phase.

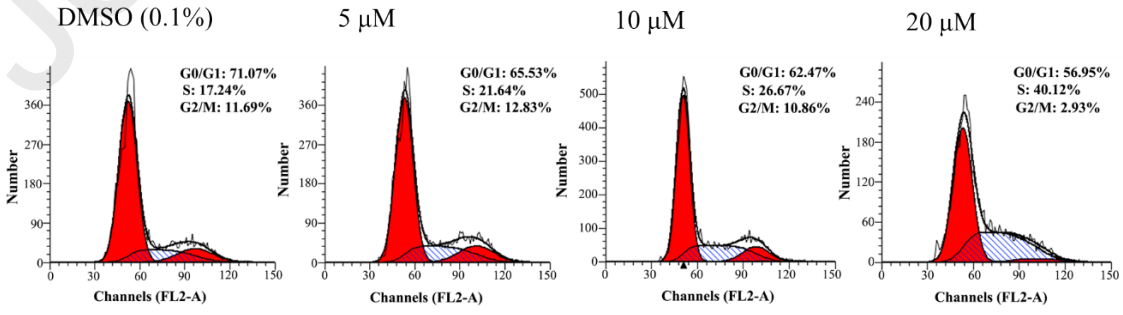

Fig. 7 Compound **22g** induces S phase arrest in HeLa cells. HeLa cells exposure to 5, 10 and 20 μM of compound **22g** for 48 h, detection and analysis of cell cycle by flow cytometry.

Cell apoptosis

Given compound **22g** could inhibit Hsp90 activity, resulting in the paramorphia of the clients including protein kinase and transcription factors associated with signals of tumor growth and metastasis. We further investigated the mechanism of compound **22g** to induce HeLa cells death using annexin-V (AV)/PI binding assay. Compared with the control group, HeLa cells treated with compounds **22g** exhibited an accumulation of early and late apoptotic cells in a time and dose dependent manner (**Fig. 8**). For example, the percentage of early apoptotic cells was 3.22% in untreated cells, while it was 17.51%, 28.57% and 38.07% in the cells treated with **22g** at 5, 10, and 20 μM for 48 h, respectively. Also, the percentage of late apoptotic cells showed similar change trend with corresponding percentages of 8.79%, 17.30% and 21.17% in cells treated with 5, 10 and 20 μM of **22g** for 48 h, respectively.

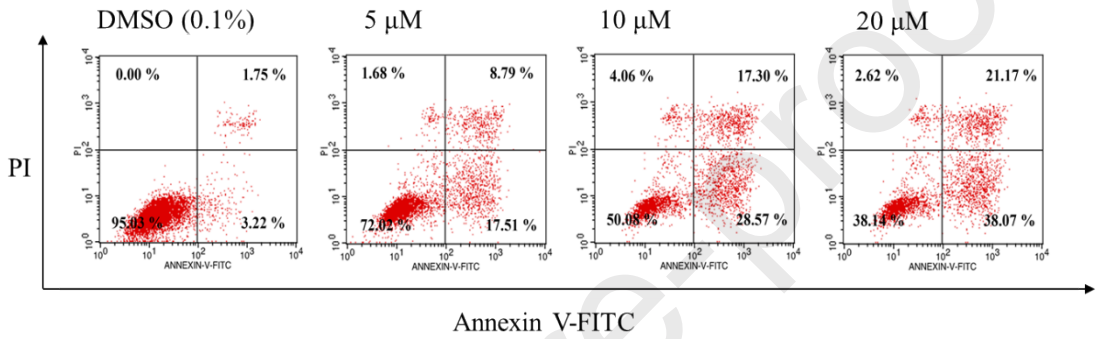

Fig. 8 Compound **22g** induced apoptosis in HeLa cells. AV/PI assay for the detection of apoptotic HeLa cells after treatment with 5, 10 and 20 μM of **22g** for 48 h.

Western bolt analysis

After treatment with compound **22g** for 48 h, the levels of apoptosis protein Bax, Bcl-2, caspase 3 and Hsp90 of HeLa cells were detected by western blotting assay. As shown in **Fig. 9**, the immunoblot results confirmed that treatment with compound **22g** decreased Bcl-2 expression, and increased Bax in a concentration-dependent manner. Moreover, the proportion of Bax/Bcl-2 increased. Additionally, caspase-3 is an executioner caspase which modifies proteins ultimately responsible for apoptosis. Consistent with the above PI-FITC/annexin assay, the results showed that the expression of cleaved caspase-3 was substantially increased, while protected caspase-3 decreased in a dose-dependent manner in HeLa cells treated with **22g**, respectively. Besides, compound **22g** performed potent binding force with Hsp90 measured by thermal shift assay and level of Hsp90 in HeLa cells was detected after their exposure to increasing concentrations of **22g**. The downregulation of Hsp90 was in accordance with the inhibition of **22g**.

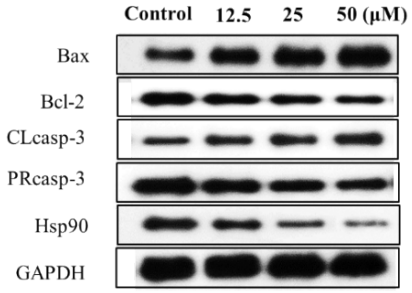

Fig. 9 HeLa cells were treated with 12.5 μM, 25 μM and 50 μM of compound **22g** or vehicle (DMSO) for 48h. As shown in the immunoblots. Cell lysates were prepared, equal amount of protein was probed with antibodies specific for Bax, Bcl-2, CLcasp-3, PRcasp-3 and Hsp90. GAPDH was used as a reference.

Conclusion

Using Hsp90 as an effective target to design inhibitors for cancer therapy enhanced antitumor potency and might help to overcome resistance. In the present study, not only is this the first design for matrine derivatives via a L-conformation transform, the results also originally verified matrine derivatives can serve as Hsp90 inhibitors. Most of L-conformation compounds **22a-22h** showed strong binding force indicated by $|\triangle Tm| > 3$ with $Hsp90^N$ and potent anticancer activity with IC_{50} below 25 μM. Besides, compound **22g** was chosen as a representative for further evaluations. Docking results indicated that the binding mode of **22g** with $Hsp90^N$ was similar to radicicol, illustrating the rationality of the design strategy. Moreover, **22g** can induce cell apoptosis, arrest the cell cycle at the S phase in HeLa cells. Western blot assay indicated that **22g** increased the expression of Bax and cleaved-caspase 3, as well as downregulated the levels Bcl-2, pro-caspase 3 and Hsp90. Taken together, all these comprehensive evaluations warranted matrine as a promising lead compound worth further optimization and development as Hsp90 inhibitors for cancer therapy.

Experimental protocols

Chemistry

Matrine was purchased from Shanxi Undersun Biomedtech Co., Ltd.- All other chemicals and reagents were obtained from Sinopharm Chemical Reagent Co., Ltd. Thin Layer Chromatography (TLC) from Yantai Xinnuo chemical Co. Ltd was used for monitoring the operation process and visualized by UV light (254 nm) or Wagner's reagent spray. Column chromatography was performed for purification on silica gel (300-400 mesh). Melting points were recorded on a WRS-1B digital melting-point apparatus without correction. ^{1}H-NMR, ^{13}C-NMR and ^{19}F-NMR spectra were recorded on a Bruker Advance 600 (600 MHz) spectrometer. Chemical shifts are reported in ppm with TMS as an internal reference and J values are given in Hertz. Signals are abbreviated as singlet, s; doublet, d; double-doublet, dd; triplet, t; quartet, q; multiplet, m. ESI-MS spectra were recorded on a WATERS UPLC I-CLASS-XEVOG2-XSQTOF electro-spray ionization mass spectrometer. Finally the optical density was measured at the 490 nm wavelength on an enzyme-linked immunosorbent assay microplate reader.

*General procedures for the synthesis of **6***

The synthetic route of intermediate **4** is described as reported by Chaojie Li et al [34]. To a solution of **4** (1g, 4 mmol) in 10% H_2SO_4 (15 mL), $KMnO_4$ (2 g) was added portion by portion in an ice bath, the reactants were then heated to reflux for 2h. After reaction completed, the solution was neutralized to pH 5~6, filtered and removed under vacuum to get crude product **5** without purification.

Acid **5** (5 mmol) and 2-chloro-1-methylpyridinium iodide (1.4g, 5.5 mmol) were dissolved in dichloromethane and 1, 4-dioxane (V:V=1:1, 150 mL), then 11mL Et_3N was added and the mixture was stirred overnight. The solvent was evaporated under vacuo to get **6**, which was then purified by

chromatograph.

Characterization of ***6***

Russet oil; yield 37%; ^{1}H NMR (600 MHz, Chloroform-*d*) δ 3.63 (dd, *J* = 10.7, 4.3 Hz, 1H), 3.48 (dd, *J* = 13.2, 6.1 Hz, 1H), 3.18 – 3.02 (m, 2H), 2.90 – 2.75 (m, 2H), 2.48 (dd, *J* = 14.4, 1.6 Hz, 1H), 2.12 (s, 1H), 1.99 – 1.85 (m, 2H), 1.87 – 1.62 (m, 4H), 1.57 – 1.39 (m, 5H), 1.31 – 1.21 (m, 1H); ^{13}C NMR (151 MHz, CDCl3) δ 166.53, 63.76, 57.66, 57.44, 44.95, 44.28, 40.96, 38.21, 35.18, 27.26, 25.68, 21.10, 20.73; HR-MS (ESI) m/z: calculated for $C_{13}H_{20}N_2O$ $[M+H]^+$: 221.1654, Found: 221.1646.

General procedures for the synthesis of ***12***

Matrine **1** (1 g, 4 mmol) was hydrolyzed by 5 N NaOH aqueous (20 mL) under reflux for overnight. After the reaction completed, the solution was cooled to room temperature followed by its acidification hydrochloric acid to pH 5~6 to gain compound 7. Subsequently, Na_2CO_3 (4g) and Fmoc-Cl (1.24 g, 4.8 mmol) in 1, 4-dioxane (20 mL) were added and stirred at room temperature for 6~8 h. Then the reaction solution was extracted with $CHCl_3$ (3 × 20 mL), the combined organic layers were dried over anhydrous $MgSO_4$ for 12 h and filtered. The solvent was evaporated under reduced pressure to get the crude product **8** in 60~70% yield without purification.

To a solution of **8** (3 mmol) in CH_2Cl_2 (10 mL), $SOCl_2$ (3.3 mL, 30 mmol) was added and the mixture was refluxed for 1~2 h under nitrogen protection. The redundant $SOCl_2$ and CH_2Cl_2 were removed through evaporation. The residue was dissolved in a small amount of CH_2Cl_2, followed by its dropwise addition to a solution of $TMSCHN_2$ (9 mmol) in CH_2Cl_2 (4.5 mL) at -15~-20 °C and the mixture was stirred for 1~2 h. After reaction completed, the mixture was washed successively with dilute acetic acid, 5% Na_2CO_3 and saturated NaCl aqueous, the combined organic layers were dried over anhydrous $MgSO_4$, filtered and evaporated to give the crude product **9**, which purified by column chromatography to gain product in 55% yield, using a mixture of CH_2Cl_2 and MeOH (30:1~40:1) as eluent.

To a solution of **9** (2 mmol) in 1, 4-dioxane (10 mL), Ag_2O (0.46g, 2 mmol), Na_2CO_3 (0.5g), $NaHSO_3$ (0.3g) and H_2O (20 mL) were added. The mixture was stirred at 50~60 °C for 2~3h. After reaction completed, dilute nitric acid was added to the reactant to adjust its pH to 5~6 and extracted with $CHCl_3$ (3 × 20 mL). The organic layer was combined, dried and evaporated to get **10** in 65% yield without purification.

Compound **10** was treated with 10% NaOH aqueous for 1~2 h at room temperature. After reaction completed, dilute hydrochloric acid was added to adjust the pH to 5~6. The solvent was evaporated to gain crude **11**. To a solution of **11** (1 mmol) in THF/DCM (V/V=1:1), HATU (1.5 mmol) and DIPEA (3 mmol) were added and the mixture was stirred overnight at room temperature. After reaction completed, the mixture was washed with dilute acidic solution, then the organic layer was combined, dried, filtered and evaporated, followed by purification with chromatograph eluted with a mixture of EA and MeOH (10:1) to gain the final target **12** in 21% yield.

Characterization of ***12***

Yellow oil; ^{1}H NMR (600 MHz, Chloroform-d) δ 4.28 – 4.22 (m, 2H), 3.96 (s, 2H), 3.21 (s, 2H), 2.84 (s, 4H), 2.58 (ddd, J = 14.9, 10.8, 4.1 Hz, 2H), 2.49 (ddd, J = 14.9, 6.9, 3.5 Hz, 2H), 2.02 – 1.30 (m, 11H), 0.93 – 0.83 (m, 1H); ^{13}C NMR (151 MHz, $CDCl_3$) δ 172.60, 67.77, 64.54, 57.08,

56.25, 45.12, 41.52, 36.41, 34.48, 29.70, 27.92, 26.74, 26.08, 22.01, 21.19, 21.06. HR-MS (ESI) m/z: calculated for $C_{16}H_{26}N_2O$ $[M+H]^+$: 263.2123, Found: 223.2121.

*General procedure for the synthesis of **21a-h**.*

Matrine **1** (1.24 g, 5 mmol) was first dissolved in DCM (30 mL) followed by the addition of $POCl_3$ (2 eq., 10 mmol) and the mixture was stirred at room temperature. When the solution color turned light yellow, the reaction mixture was placed in an oil bath at 60 °C and stirred for 2-3 h until the solution turned brown. It was then cooled to room temperature and the corresponding aniline (1-1.5 eq.) dissolved in DCM was added dropwise, followed by reflux for 12 h at 60 °C. After reaction completion, NaOH aqueous was added to adjust the pH to 8-9. The mixture was then extracted with DCM (3 × 20 mL). The organic layers were collected, dried over $MgSO_4$, and concentrated under vacuo. The crude product was purified by column chromatography using PE: DCM = 5:1 to DCM: EA = 1:1 as eluents.

*(E)-15-(N-phenyl) matrinic imine (**21a**).*

Yellow powder; yield 73%; mp: 116.8-117.6 °C; ^{1}H NMR (600 MHz, Chloroform-*d*) δ 7.25 – 7.16 (m, 2H, Ar-H), 6.96 – 6.87 (m, 1H, Ar-H), 6.73 – 6.67 (m, 2H, Ar-H), 4.39 (dd, *J* = 12.9, 4.5 Hz, 1H, H-17α), 3.70 (m, 1H, H-11), 3.16 (t, *J* = 12.7 Hz, 1H, H-17β), 2.86 – 2.79 (m, 2H), 2.40 (m, 1H), 2.10 (t, *J* = 3.1 Hz, 1H, H-6), 2.09 – 2.00 (m, 2H), 1.99 – 1.89 (m, 3H), 1.89 – 1.76 (m, 2H), 1.73 – 1.61 (m, 3H), 1.52 (m, 2H), 1.50 – 1.25 (m, 5H); ^{13}C NMR (151 MHz, $CDCl_3$) δ 157.78, 151.89, 128.60, 122.33, 121.15, 64.14, 57.44, 57.33, 53.78, 43.78, 42.94, 34.68, 27.99, 27.79, 27.38, 26.70, 21.37, 20.99, 19.98; HR-MS (ESI) m/z: calculated for $C_{21}H_{30}N_3$ $[M+H]^+$: 324.2434, Found: 324.2432.

*(E)-15-(N-4-chlorophenyl) matrinic imine (**21b**).*

White powder; yield 57%; mp: 106.4-107.9 °C; ^{1}H NMR (600 MHz, Chloroform-d) δ 7.21 – 7.14 (m, 2H), 6.72 – 6.61 (m, 2H), 4.38 (dd, J = 12.8, 4.5 Hz, 1H), 3.72 (m, 1H), 3.16 (t, J = 12.7 Hz, 1H), 2.84 (m, 2H), 2.38 (m, 1H), 2.12 (t, J = 3.1 Hz, 1H), 2.11 – 2.01 (m, 2H), 2.01 – 1.91 (m, 3H), 1.90 – 1.74 (m, 2H), 1.75 – 1.61 (m, 3H), 1.54 (m, 2H), 1.50 – 1.21 (m, 5H). ^{13}C NMR (151 MHz, CDCl3) δ 158.00, 150.57, 128.59, 126.19, 123.66, 64.08, 57.41, 57.30, 53.73, 43.74, 42.99, 34.71, 27.95, 27.70, 27.40, 26.66, 21.34, 20.95, 19.79; HR-MS (ESI) m/z: calculated for $C_{21}H_{29}N_3Cl$ $[M+H]^+$: 358.2045, Found: 358.2044.

*(E)-15-(N-4-ethoxyphenyl) matrinic imine (**21c**).*

Brown solid; yield 55%; mp:107.2-110.2 °C; ^{1}H NMR (600 MHz, Chloroform-*d*) δ 6.79 – 6.74 (m, 2H, Ar-H), 6.67 – 6.56 (m, 2H, Ar-H), 4.38 (dd, *J* = 12.9, 4.5 Hz, 1H, H-17α), 3.98 (q, *J* = 7.0 Hz, 2H, OCH_2), 3.75 – 3.61 (m, 1H, H-11), 3.14 (t, *J* = 12.7 Hz, 1H, H-17β), 2.83 (m, 2H), 2.41 (m, 1H), 2.10 (t, *J* = 3.1 Hz, 1H, H-6), 2.09 – 1.99 (m, 2H), 1.99 – 1.88 (m, 3H), 1.88 – 1.72 (m, 2H), 1.72 – 1.57 (m, 3H), 1.52 (m, 2H), 1.45 – 1.34 (m, 8H, CH, CH_2, CH_3); ^{13}C NMR (151 MHz, $CDCl_3$) δ 158.55, 153.82, 144.99, 122.99 (2), 114.76 (2), 64.16, 63.64, 57.43, 57.32, 53.81, 43.78, 42.95, 34.68, 27.95, 27.80, 27.33, 26.69, 21.36, 20.97, 19.97, 15.00; HR-MS (ESI) m/z: calculated for $C_{23}H_{34}N_3O$ $[M+H]^+$: 368.2696, Found: 368.2694.

*(E)-15-(N-4-isopropylphenyl) matrinic imine (**21d**).*

Yellow solid; yield 69%; mp: 134.1-135.6 °C; ^{1}H NMR (600 MHz, Chloroform-*d*) δ 7.20 – 6.94 (m, 2H , Ar-H), 6.78 – 6.33 (m, 2H, Ar-H), 4.39 (dd, *J* = 12.9, 4.5 Hz, 1H, H-17α), 3.70 (m, 1H, H-11), 3.15 (t, *J* = 12.7 Hz, 1H, H-17β), 2.90 – 2.79 (m, 3H), 2.45 (m, 1H), 2.12 (t, *J* = 3.1 Hz, 1H, H-6), 2.11 – 2.00 (m, 2H), 2.00 – 1.91 (m, 3H), 1.91 – 1.75 (m, 2H), 1.76 – 1.58 (m, 3H), 1.54 (m, 2H), 1.42 (m, 5H), 1.23 (d, *J* = 6.9 Hz, 6H, 2CH_3); ^{13}C NMR (151 MHz, $CDCl_3$) δ 157.96, 149.30, 141.55, 126.50 (2), 122.04 (2), 64.21, 57.45, 57.35, 53.82, 43.82, 42.94, 34.67, 33.39, 27.98, 27.83, 27.38, 26.71, 24.23, 24.21, 21.38, 20.99, 20.01; HR-MS (ESI) m/z: calculated for $C_{24}H_{36}N_3$ [M+H] $^{+}$: 366.2904, Found: 366.2903.

*(E)-15-(N-4-biphenyl) matrinic imine (**21e**).*

Brown oil; yield 49%; ^{1}H NMR (600 MHz, Chloroform-*d*) δ 7.64 – 7.59 (m, 2H, Ar-H), 7.52 – 7.47 (m, 2H, Ar-H), 7.42 (t, *J* = 7.7 Hz, 2H, Ar-H), 7.33 – 7.24 (m, 1H , Ar-H), 6.81 (d, *J* = 8.1 Hz, 2H, Ar-H), 4.45 (dd, *J* = 12.9, 4.5 Hz, 1H, H-17α), 3.76 (m, 1H, H-11), 3.21 (t, *J* = 12.7 Hz, 1H, H-17β), 2.95 – 2.81 (m, 2H), 2.50 (m, 1H), 2.19 – 2.08 (m, 3H), 2.06 – 1.80 (m, 5H), 1.80 – 1.63 (m, 3H), 1.61 – 1.52 (m, 2H), 1.52 – 1.25 (m, 5H); ^{13}C NMR (151 MHz, $CDCl_3$) δ 157.92, 141.31, 134.01, 128.60 (2), 127.32 (2), 126.58 (2), 126.36 (2), 122.80, 118.43, 64.16, 57.43, 57.34, 53.84, 43.89, 43.01, 34.75, 27.96, 27.77, 27.54, 26.69, 21.36, 20.98, 19.88; HR-MS (ESI) m/z: calculated for $C_{24}H_{36}N_3$ [M+H] $^{+}$: 400.3457, Found: 400.3462.

*(E)-15-(N-4-phenoxyphenyl) matrinic imine (**21f**).*

White powder; yield 58%; mp: 132.0-132.3 °C; ^{1}H NMR (600 MHz, Chloroform-*d*) δ 7.34 – 7.24 (m, 2H, Ar-H), 7.09 – 7.01 (m, 1H, Ar-H), 7.00 – 6.95 (m, 2H, Ar-H), 6.95 – 6.86 (m, 2H, Ar-H), 6.74 – 6.66 (m, 2H, Ar-H), 4.41 (dd, *J* = 12.9, 4.5 Hz, 1H, H-17α), 3.73 (m, 1H, H-11), 3.18 (t, *J* = 12.7 Hz, 1H, H-17β), 2.86 (m, 2H), 2.47 (m, 1H), 2.11 (m, 3H), 2.05 – 1.92 (m, 3H), 1.85 (m, 2H), 1.76 – 1.68 (m, 3H), 1.54 (m, 2H), 1.51 – 1.22 (m, 5H); ^{13}C NMR (151 MHz, $CDCl_3$) δ 158.72, 158.27, 150.81, 147.95, 129.49 (2), 123.35, 122.12 (2), 120.26 (2), 117.52 (2), 64.15, 57.44, 57.33, 53.81, 43.80, 42.98, 34.70, 27.97, 27.78, 27.40, 26.69, 21.36, 20.98, 19.94; HR-MS (ESI) m/z: calculated for $C_{27}H_{34}N_3O$ [M+H] $^{+}$: 416.2696, Found: 416.2694.

*(E)-15-(N-2-methyl-3-nitrophenyl) matrinic imine (**21g**).*

Yellow crystals; yield 84%; m.p: 124.0-124.9 °C; ^{1}H NMR (600 MHz, Chloroform-*d*) δ 7.40 (dd, *J* = 8.1, 1.2 Hz, 1H, Ar-H), 7.14 (t, *J* = 8.0 Hz, 1H, Ar-H), 6.84 (dd, *J* = 7.9, 1.2 Hz, 1H, Ar-H), 4.42 (dd, *J* = 12.9, 4.5 Hz, 1H, H-17α), 3.78 (m, 1H, H-11), 3.22 (t, *J* = 12.7 Hz, 1H, H-17β), 2.90 – 2.81 (m, 2H), 2.23 (s, 3H, CH_3), 2.19 (m, 1H), 2.15 (d, *J* = 3.1 Hz, 1H, H-6), 2.12 – 1.91 (m, 5H), 1.90 – 1.60 (m, 5H), 1.60 – 1.52 (m, 2H), 1.51 – 1.20 (m, 5H); ^{13}C NMR (151 MHz, $CDCl_3$) δ 157.67, 152.58, 151.21, 126.00, 125.97, 124.35, 116.95, 64.08, 57.38, 57.29, 53.76, 43.95, 42.86, 34.77, 27.94, 27.58, 27.43, 26.63, 21.31, 20.91, 19.51, 13.86; HR-MS (ESI) m/z: calculated for $C_{22}H_{31}N_4O_2$ [M+H] $^{+}$: 383.2442, Found: 383.2439.

*(E)-15-(N-2-cyanophenyl) matrinic imine (**21h**).*

Colorless crystals; yield 79%; mp:135.9-136.6 °C; ^{1}H NMR (600 MHz, Chloroform-*d*) δ 7.36 (t, *J* = 6.1 Hz, 1H, Ar-H), 7.27 (t, *J* = 7.6 Hz, 1H, Ar-H), 6.80 (m, 1H, Ar-H), 6.68 (dd, *J* = 8.7, 3.7 Hz, 1H, Ar-H), 4.36 (m, 1H, H-17α), 3.73 (m, 1H, H-11), 3.11 (m, 1H, H-17β), 2.83 – 2.54 (m, 2H), 2.17 (m, 1H), 2.03 (m, 2H), 1.98 – 1.91 (m, 1H), 1.91 – 1.78 (m, 3H), 1.78 – 1.53 (m, 4H), 1.53 –

1.40 (m, 2H), 1.32 (m, 6H); ^{13}C NMR (151 MHz, $CDCl_3$) δ 157.63, 155.78, 133.01, 132.52, 123.14, 120.86, 118.51, 105.58, 63.97, 57.25, 57.18, 53.40, 44.02, 42.72, 34.50, 27.88, 27.41, 26.93, 26.48, 21.23, 20.81, 18.85; HR-MS (ESI) m/z: calculated for $C_{22}H_{29}N_4$ $[M+H]^+$: 349.2387, Found: 349.2388.

*General procedure for the synthesis of **20a-h**.*

Matrine **1** (1.24 g, 5 mmol) dissolved in DCM (30 mL) was treated with $POCl_3$ (2 eq., 10 mmol) at room temperature. When color of the reaction mixture turned yellow, it was then stirred at 60 °C for 2-3 h. The solution was then cooled to room temperature and the corresponding aniline bearing cyan derivatives **18a-h** (1-1.5 eq.) dissolved in DCM were added dropwise, followed by reflux for 12 h at 60 **°C**. After reaction completion, NaOH aqueous was added to adjust the pH to 8-9. The mixture was then extracted with DCM (3 × 20 mL). The organic layers were collected, dried over $MgSO_4$, and concentrated. The residue was purified by column chromatography to obtain product **20a-h**.

*General procedure for the synthesis of **22a-h**.*

Compound **20a-h** (2 mmol) was dissolved in dry THF (30 mL), followed by the addition of LDA (3eq.). The mixture was stirred at 0 °C and reaction progress was monitored by TLC analysis. After completion of the reaction, the mixture solution was quenched with saturated ammonium chloride solution and extracted with DCM (3 × 20 mL). The organic layers were combined, concentrated and the residue was purified by column chromatography on silica gel using EA: MeOH= 9: 1 as eluent or on alumina using PE: EA= 5: 1 as eluent to afford **22a-h**.

*4-amino-quinolinomatrine (**22a**).*

Yellow powder; yield 53%; mp: 197.0-197.2 °C; ^{1}H NMR (600 MHz, Chloroform-*d*) δ 7.61 (d, *J* = 8.3 Hz, 1H, Ar-H), 7.49 (dd, *J* = 8.2, 1.4 Hz, 1H, Ar-H), 7.43 (m, 1H, Ar-H), 7.19 – 6.99 (m, 1H, Ar-H), 4.92 (dd, *J* = 12.7, 4.5 Hz, 1H, H-17α), 4.33 (s, 2H, NH_2), 3.94 (m, 1H, H-11), 3.34 (t, *J* = 12.6 Hz, 1H, H-17β), 2.86 (m, 2H), 2.65 – 2.45 (m, 2H), 2.31 – 2.10 (m, 2H), 2.05 – 1.72 (m, 8H), 1.61 (m, 1H), 1.58 – 1.35 (m, 4H); ^{13}C NMR (151 MHz, $CDCl_3$) δ 155.78, 147.16, 144.76, 128.32, 126.74, 120.44, 119.40, 115.07, 99.18, 64.45, 57.56, 57.46, 51.56, 45.01, 39.68, 34.98, 28.10, 26.59, 23.24, 21.54, 21.14, 19.47; HR-MS (ESI) m/z: calculated for $C_{22}H_{29}N_4$ $[M+H]^+$: 349.2387, Found: 349.2385.

*4-amino-6-methylquinolinomatrine (**22b**).*

Yellow powder; yield 55%; mp: 182.1-184.5 °C; ^{1}H NMR (600 MHz, Chloroform-*d*) δ 7.53 (d, *J* = 8.9 Hz, 1H, Ar-H), 7.35 – 7.06 (m, 2H, Ar-H), 4.89 (dd, *J* = 12.8, 4.5 Hz, 1H, H-17α), 4.30 (s, 2H, NH_2), 3.92 (m, 1H, H-11), 3.33 (t, *J* = 12.6 Hz, 1H, H-17β), 2.86 (m, 2H), 2.56 (m, 2H), 2.45 (s, 3H, CH_3), 2.26 – 2.12 (m, 2H), 2.02 – 1.69 (m, 8H), 1.64 – 1.35 (m, 5H); ^{13}C NMR (151 MHz, $CDCl_3$) δ 155.40, 145.37, 144.38, 130.21, 129.77, 126.62, 118.75, 114.83, 99.31, 64.47, 57.58, 57.47, 51.57, 45.02, 39.70, 34.91, 28.11, 26.62, 23.40, 21.55, 21.48, 21.16, 19.61; HR-MS (ESI) m/z: calculated for $C_{23}H_{31}N_4$ $[M+H]^+$: 363.2543, Found: 363.2545.

*4-amino-6-methoxyquinolinomatrine (**22c**).*

Brown solid; yield 35%; mp: 103.2-105.3 °C; ^{1}H NMR (600 MHz, Chloroform-*d*) δ 7.58 (d, *J* = 9.1

Hz, 1H, Ar-H), 7.13 (dd, *J* = 9.1, 2.7 Hz, 1H, Ar-H), 6.86 (d, *J* = 2.8 Hz, 1H, Ar-H), 4.83 (dd, *J* = 12.8, 4.4 Hz, 1H, H-17α), 4.29 (s, 2H, NH_2), 3.90 (m, 1H, H-11), 3.88 (s, 3H, OCH_3), 3.33 (t, *J* = 12.6 Hz, 1H, H-17β), 2.86 (m, 2H), 2.56 (m, 2H), 2.34 – 2.10 (m, 2H), 2.05 – 1.69 (m, 8H), 1.68 – 1.35 (m, 5H); ^{13}C NMR (151 MHz, $CDCl_3$) δ 154.58, 154.04, 144.28, 142.33, 128.14, 119.05, 115.00, 100.12, 99.82, 64.43, 57.56, 57.46, 55.67, 51.59, 45.10, 39.69, 34.85, 28.10, 26.62, 23.45, 21.54, 21.15, 19.72; HR-MS (ESI) m/z: calculated for $C_{23}H_{31}N_4O$ $[M+H]^+$: 379.2492, Found: 379.2491.

*4-amino-6-fluoroquinolinomatrine (**22d**).*

Brown solid; yield 33%; mp: 199.3-202.8 °C; ^{1}H NMR (600 MHz, Chloroform-*d*) δ 7.58 (dd, *J* = 9.1, 5.4 Hz, 1H, Ar-H), 7.20 (t, *J* = 8.9 Hz, 1H, Ar-H), 7.14 (d, *J* = 9.8 Hz, 1H, Ar-H), 4.85 (dd, *J* = 12.7, 4.4 Hz, 1H, H-17α), 4.24 (s, 2H, NH_2), 3.94 (m, 1H, H-11), 3.34 (t, *J* = 12.6 Hz, 1H, H-17β), 2.87 (dd, *J* = 32.8, 11.2 Hz, 2H), 2.57 (m, 2H), 2.29 – 2.12 (m, 2H), 2.03 – 1.73 (m, 8H), 1.63 – 1.36 (m, 5H); ^{13}C NMR (151 MHz, Chloroform-*d*) δ 157.42 (d, *J* = 239.3 Hz, F-Ar-C), 155.39, 144.30, 143.97, 128.56, 117.43, 114.94, 103.76, 100.07, 64.40, 57.53, 57.43, 51.53, 44.97, 39.73, 34.93, 28.09, 26.58, 23.24, 21.51, 21.11, 19.58; ^{19}F NMR (565 MHz, $CDCl_3$) δ -121.80; HR-MS (ESI) m/z: calculated for $C_{22}H_{28}N_4F$ $[M+H]^+$: 367.2293, Found: 367.2296.

*4-amino-6-chloroquinolinomatrine (**22e**).*

Brown solid, yield 39%; mp: carbonized; ^{1}H NMR (600 MHz, Chloroform-*d*) δ 7.53 (d, *J* = 8.9 Hz, 1H, Ar-H), 7.46 (d, *J* = 2.3 Hz, 1H, Ar-H), 7.35 (dd, *J* = 8.9, 2.3 Hz, 1H, Ar-H), 4.87 (dd, *J* = 12.8, 4.5 Hz, 1H, H-17α), 4.27 (s, 2H, NH_2), 3.95 (m, 1H, H-11), 3.34 (t, *J* = 12.6 Hz, 1H, H-17β), 2.87 (m, 2H), 2.72 – 2.48 (m, 2H), 2.29 – 2.10 (m, 2H), 2.02 – 1.72 (m, 8H), 1.64 – 1.39 (m, 5H); ^{13}C NMR (151 MHz, $CDCl_3$) δ 155.86, 145.68, 143.93, 128.77, 128.23, 125.47, 118.89, 115.78, 99.93, 64.36, 57.52, 57.42, 51.53, 44.94, 39.77, 35.03, 28.07, 26.56, 23.11, 21.50, 21.09, 19.46; HR-MS (ESI) m/z: calculated for $C_{22}H_{28}N_4Cl$ $[M+H]^+$: 383.1997, Found: 383.1998.

*4-amino-6-bromoquinolinomatrine (**22f**).*

White powder; yield 41%; mp: carbonized; ^{1}H NMR (600 MHz, Chloroform-*d*) δ 7.61 – 7.50 (m, 1H, Ar-H), 7.27 (dd, *J* = 8.9, 2.4 Hz, 1H, Ar-H), 7.09 (d, *J* = 2.3 Hz, 1H, Ar-H), 4.90 (dd, *J* = 12.8, 4.4 Hz, 1H, H-17α), 4.33 (s, 2H, NH_2), 3.93 (m, 1H, H-11), 3.34 (t, *J* = 12.6 Hz, 1H, H-17β), 2.86 (m, 2H), 2.57 (m, 2H), 2.30 – 2.09 (m, 2H), 2.08 – 1.93 (m, 3H), 1.94 – 1.67 (m, 5H), 1.66 – 1.38 (m, 5H); ^{13}C NMR (151 MHz, $CDCl_3$) δ 155.02, 154.78, 144.48, 140.42, 128.23, 125.97, 116.19, 114.58, 99.12, 64.47, 57.57, 57.46, 51.67, 48.56, 39.75, 34.97, 28.08, 26.62, 23.39, 21.54, 21.15, 19.59; HR-MS (ESI) m/z: calculated for $C_{22}H_{28}N_4Br$ $[M+H]^+$: 427.1492, Found: 427.1495.

*4-amino-6-trifluoromethylquinolinomatrine (**22g**).*

Yellow powder; yield 65%; mp: carbonized; ^{1}H NMR (600 MHz, Chloroform-*d*) δ 7.77 (d, *J* = 1.9 Hz, 1H, Ar-H), 7.63 (d, *J* = 8.8 Hz, 1H, Ar-H), 7.59 (dd, *J* = 8.8, 1.9 Hz, 1H, Ar-H), 4.93 (dd, *J* = 12.8, 4.5 Hz, 1H, H-17α), 4.40 (s, 2H, NH_2), 3.99 (m, 1H, H-11), 3.36 (t, *J* = 12.6 Hz, 1H, H-17β), 2.86 (m, 2H), 2.69 – 2.46 (m, 2H), 2.30 – 2.11 (m, 2H), 2.03 – 1.69 (m, 8H), 1.66 – 1.37 (m, 5H); ^{13}C NMR (151 MHz, $CDCl_3$) δ 156.81, 148.97, 144.96, 127.16, 124.96, 124.21, 121.62 (q, *J* = 32.2 Hz), 117.58, 114.07, 99.84, 64.30, 57.49, 57.39, 51.57, 44.97, 39.80, 35.20, 28.05, 26.51, 22.85, 21.47, 21.05, 19.26. ^{19}F NMR (565 MHz, $CDCl_3$) δ -61.10; HR-MS (ESI) m/z: calculated for

$C_{23}H_{28}N_4F_3$ $[M+H]^+$: 417.2261, Found: 417.2262.

*4-amino-6-nitroquinolinomatrine (**6h**).*

Brown powder; yield 39%; mp: carbonized; ^{1}H NMR (600 MHz, Chloroform-*d*) δ 8.54 (d, *J* = 2.5 Hz, 1H, Ar-H), 8.19 (dd, *J* = 9.2, 2.5 Hz, 1H, Ar-H), 7.51 (d, *J* = 9.3 Hz, 1H, Ar-H), 4.96 (dd, *J* = 12.8, 4.5 Hz, 1H, H-17α), 4.57 (s, 2H,NH_2), 4.10 – 3.96 (m, 1H, H-11), 3.39 (t, *J* = 12.6 Hz, 1H, H-17β), 2.87 (m, 2H), 2.66 – 2.44 (m, 2H), 2.22 – 2.13 (m, 2H), 2.08 – 1.70 (m, 8H), 1.67 – 1.39 (m, 5H); ^{13}C NMR (151 MHz, $CDCl_3$) δ 157.44, 151.32, 145.64, 140.09, 126.84, 122.77, 117.71, 113.63, 99.68, 64.17, 57.42, 57.34, 51.78, 45.07, 40.01, 35.58, 27.99, 26.45, 22.45, 21.41, 20.97, 18.97; HR-MS (ESI) m/z: calculated for $C_{22}H_{28}N_5O_2$ $[M+H]^+$: 394.2238, Found: 394.2235.

Thermal shift assay

Mix $Hsp90^N$ protein, buffer, compounds dissolved in DMSO (if applicable) and PTS dye in a 20 μL reaction system. The molar ratio of protein to ligand is 1:5. Then run a melt-curve experiment on a real-time PCR instrument (7500, ABI Company, USA). Plates were run from 25 °C to 95 °C with a ramp rate of 1 °C/min. The protein unfolds as it is heated and the environmentally-sensitive PTS dye binds exposed hydrophobic regions and fluoresces. The melting temperature (Tm) was calculated from the melt curve and ΔTm was correlated to changes in protein stability or ligand binding.

Anticancer activity assay in vitro

HepG2 and HeLa cell lines were obtained from the American Type Culture Collection (ATTC). The cells were prepared in DMEM supplemented with 10% fetal bovine serum (FBS) and 1% penicillin-streptomycin and were then cultured in 96-well plates. After a 24 h incubation period in 5% CO_2 at 37 °C, compounds with different concentrations (1, 5, 10, 20, 50 and 100 μM) made by serial dilution in culture medium of stock solutions of test compounds prepared in DMSO, were added and incubated for 48 h. Then, 20 μL MTT (5 mg/mL) was added to each well and the wells were incubated for 4 h. Supernatant from each well was carefully removed and 150 μL DMSO was added to each well for the colorimetric reaction. Finally, the absorbance was detected at 490 nm wavelength on an enzyme-linked immunosorbent assay microplate reader and each concentration was tested in threefold.

Docking

The chemical structures were constructed on the sketch module of Sybyl 21.0 software (Tripos Company, USA). The molecular modeling studies require the minimization of structure, calculation of the force field and charges. The energy minimization and charge calculation done by Tripos force field and Pullman charge (or other) respectively. Human $Hsp90^N$ structure (PDB ID: 1UYM) downloaded from Protein Data Bank was utilized in docking, ligands and water molecules were removed, polar hydrogen atoms, charges were added and energy minimization executed. The Surflex-Dock module used to dock ligands into a ligand-protein's extracted binding site. The protomol bloat value was set as 1 and the protomol threshold value as 0.5 to obtained meaningful binding pocket. Other parameters are established by default in software.

Cell apoptosis

For Annexin V-propidium iodide assay, HeLa cells were seeded in a six-well plates in a density of 2×10^5 cells per well, incubated overnight and then treated with graded concentrations of compound **22g** for 48 h. Cellular apoptosis was determined by annexin V-PI apoptosis detection kit (Beyotime, CN) following its instructions Cells in early or late apoptotic phases were represented as cumulative percentage compared with control.

Cell cycle

HeLa cells were treated with certain concentrations of compound 22g for 48 h. The cells were then collected, washed, and fixed with 75% ethanol for 24 h at 4 °C. The cells were then stained with 4 mg/mL PI and 0.1 mg/mL RNaseA for 30 min in the dark. After staining, cell cycle distribution of 10,000 cells from each group was analyzed using an Aria FACS flow cytometry system (Bection Dickinson, USA).

Western boltting

HeLa cells were treated with different concentrations of compound 22g, the cells were collected, lysed in RIPA buffer containing a protease inhibitor cocktail for 30 min, followed by centrifugation at 12,000 rpm for 15 min at 4 ℃. Proteins were subjected to 6-15% SDS-PAGE, electrophoresed and transferred on to a nitrocellulose membrane. After blocking with 5% non-fat milk in Tris-buffered saline, the membrane was washed and incubated with the indicated primary and secondary antibodies and detected using the syngene (G:BOXChemiXR5, UK).

Conflict of interest

The authors declare no conflict of interest.

Acknowledgments

This work was supported by Innovation Project of Guangxi Graduate Education (YCBZ2019026), the National Natural Science Foundation of China (21403225, U1932130), the Talents Program of Xi'an Medical University (2015RCYJ01), the Key Program of Shaanxi Provincial Science and Technology Department (2017ZDXM-SF-029); the Key Program of Shaanxi Provincial Education Department (18JS102).

Reference

[1] Kyogoku, K.; Hatayama, K.; and Komatsu, M. Constituents of a Chinese crude drug Kushen (the root of Sophora flavescens). Isolation of five new flavonoids and formononetin. Chem. Pharm. Bull., 1973, 21, 2733.

[2] Wang, C. Y.; Bai, X. Y.; Wang, C. H. Traditional Chinese medicine: a treasured natural resource of anticancer drug research and development, Am. J. Chin. Med., 2014, 42, 543-559.

[3] Choudhary, M. I.; Parvez, K.; Ahmed, A.; Akhtar, F.; Nur-e-Alam, M.; Hassan, N. M. Quinolizidine alkaloids from Sophora alopecuroides, J. Nat. Prod., 2000, 63, 190-192.

[4] Liu, Y.; Xu, Y.; Ji, W.; Li, X.; Sun, B.; Gao, Q.; Su, C. Anti-tumor activities of matrine and oxymatrine: literature review, Tumor Biol., 2014, 35, 5111-5119.

[5] Zhao, Z.; Fan, H.; and Higgins, T. Fufang Kushen injection inhibits sarcoma growth and tumor-induced hyperalgesia via TRPV1 signaling pathways. Cancer Lett., 2014, 355, 232-241.

[6] Zhou, S. K.; Zhang, R. L; Xu, Y. F.; Qi, J.; Haines, D.; Trivett, A.; Oppenheim, J. J.; Wei, H.; Li, J.; Lin, H. S.; and Howard, O. M. Z. Antioxidant and immunity activities of Fufang Kushen Injection Liquid. Molecules, 2012, 17, 6481-6490.

[7] Luo, C.; Zhong, H. J.; Zhu, L. M.; Wu, X. G.; Ying, J. E.; Wang, X. H.; Lü, W. X.; Xu, Q.; Zhu, Y. L.; Huang, J. Inhibition of matrine against gastric cancer cell line MNK45 growth and its anti-tumor mechanism, Mol. Biol. Rep., 2012, 39, 5459-5464.

[8] Zhang, Y.; Zhang, H.; Yu, P.; Liu, Q.; Liu, K.; Duan, H.; Luan, G.; Yagasaki, K.; Zhang, G. Effects of matrine against the growth of human lung cancer and hepatoma cells as well as lung cancer cell migration, Cytotechnology, 2009, 59, 191-200.

[9] Zhang, L.; Jiang, J.; Tam, J.; Zhang, Y.; Liu, X.; Xu, X.; Liu, B.; He, Y. Effects of matrine on proliferation and differentiation in K-562 cells, Leuk. Res., 2001, 25, 793-800.

[10] Chui, C. H.; Lau, F.Y.; Tang, J. C. O.; Kan, K.L.; Cheng, G. Y. M.; Wong, R. S. M.; Kok, S. H. L.; Lai, P. B. S.; Ho, R.; Gambari, R. Activities of fresh juice of Scutellaria barbata and warmed water extract of Radix Sophorae Tonkinensis on antiproliferation and apoptosis of human cancer cell lines, Int. J. Mol. Med., 2005,16, 337-341.

[11] Zhang, S.; Qi, J.; Sun, L.; Cheng, B.; Pan, S.; Zhou, M.; Sun, X. Matrine induces programmed cell death and regulates expression of relevant genes based on PCR array analysis in C6 glioma cells, Mol. Biol. Rep., 2009, 36, 791-799.

[12] Rashid, H. U.; Xu, Y. M., Muhammad, Y.; Wang, L. S.; Jiang, J. Research advances on anticancer activities of matrine and its derivatives: An updated overview. Eur. J. Med. Chem., 2019, 161, 205-238.

[13] Maloney, A.; Workman, P. Hsp90 as a new therapeutic target for cancer therapy: the story unfolds [J]. Expert Opin Biol Ther, 2002, 2, 3-24.

[14] Dymock, B. W.; Drysdale, M. J.; McDonald, E.; Workman, P. Inhibitors of HSP90 and other chaperones for the treatment of cancer. Expert Opin. Ther. Pat., 2004, 14, 837-847.

[15] Banerji, U.; Judson, I.; Workman, P. The clinical applications of heat shock protein inhibitors in cancer - present and future. Curr. Cancer Drug Targets, 2003, 3, 385-390.

[16] Stebbins, C. E.; Russo, A. A.; Schneider, C. et al. Crystal structure of an Hsp90-geldanamycin complex; targeting of a protein chaperone by an antitumor agent[J]. Cell, 1997, 89, 239-250.

[17] Obermann, W. M.; Sondermann, H.; Russo, A. A. et al. In vivo function of hsp90 is dependent on ATP binding and ATP hydrolysis[J]. J. Cell. Biol., 1998, 143, 901-910.

[18] Roe, S. M.; Prodromou, C.; O'Brien, R.; Ladbury, J. E.; Piper, P. W.; Pearl, L. H. Improved procedure for the synthesis of methyl ethers from alcohols. J. Med. Chem., 1999, 42, 260-266.

[19] Li, C. J.; Liu, Y. X.; Wang, Q. M. Controllable and efficient oxidation of thioether by 2-iodoxybenzoic acid (IBX) in water: semisynthesis of sophocarpine. Tetrahedron Lett., 2014, 55, 950-953.

[20] Huang, H. M.; Iwasawa, N.; Mukaiyama, T. A convenient method for the construction of β-lactam compounds from β-amino acids using 2-chloro-1-methylpyridinium iodide as condensing reagent. Chem. Lett., 1984, 1465-1466.

[21] Kirmse, W. (2002). "100 Years of the Wolff Rearrangement". Eur. J. Org. Chem., 2002, 14, 2193.

[22] Archiv der Pharmazie und Berichte der Deutschen Pharmazeutischen Gesellschaft. Condensed 2-azetidinones. I. 1-Azabicyclo[4.2.0]octan-2-one. Arch. Pharm. Weinheim., 1968, 301, 230-238.

[23] Hassan, H.; Mohammed, S.; Robert, F.; Landais, Y. Total Synthesis of (±)-Eucophylline. A

Free-Radical Approach to the Synthesis of the Azabicyclo[3.3.1]nonane Skeleton. Org. Lett., 2015, 17, 4518-4521.

[24] Capilla, J.; Serena, C.; Pastor, F. J.; Ortoneda, M.; Guarro, J. Efficacy of voriconazole in treatment of systemic scedosporiosis in neutropenic mice. Antimicrob. Agents Chemother., 2003, 47, 3976-3978.

[25] Bawa, S.; Kumar, S.; Drabu, S.; Kumar, R. Synthesis and antimicrobial activity of 2-chloro-6-methylquinoline hydrazone derivatives. J. Pharm. Bioallied Sci., 2009, 1, 27-31.

[26] Minami, M.; Togashi, H.; Sano, M.; Saito, I.; Morii, K.; Nomura, A.; Kurosawa, M.; Yoshioka, M.; Saito, H. Effect of metoprolol on water drinking activity in Wistar Kyoto rats. Hokkaido Igaku Zasshi., 1984, 59, 471-477.

[27] Todeschini, A. R.; De Miranda, A. L. P.; Da S.; Kelly C. M.; Parrini, S. C.; Barreiro, E. J. Synthesis and evaluation of analgesic, antiinflammatory and antiplatelet properties of new 2-pyridyl aryl hydrazone derivatives. Eur. J. Med. Chem., 1998, 33, 189-199.

[28] Ali, I.; Haque, A.; Saleem, K.; Hsieh, M. F. Curcumin-I Knoevenagel's condensates and their Schiff's bases as anticancer agents: Synthesis, pharmacological and simulation studies. Bioorg. Med. Chem., 2013, 21, 3808-3820.

[29] Shashikala, M.; Arunadevi, P.; Sarangapani, M.; Prasad, M. S. K. Metal based Schiff bases as anticancer agents. Eur. J. Pharm. Sci., 2016, 3, 118-121.

[30] Utreja, D.; Vibha; Singh, S.; Kaur, M. Schiff Bases and their Metal Complexes as Anti-Cancer Agents: A Review. Current Bioactive Compounds., 2015, 11, 215-230.

[31] Daniel, M. M.; Rozbeh J.; Marina I.; Takahiro S.; E. Andreas L.; Chen D.; Lekshmy S.; Yihai C.; Pär N. Monitoring Drug Target Engagement in Cells and Tissues Using the Cellular Thermal Shift Assay. Science, 2013, 341, 84-87.

[32] Lo, M.; Aulabaugh, A.; Jin, G.; Cowling, R.; Bard, J.; Malamas, M.; Ellestad, G. Evaluation of fluorescence-based thermal shift assays for hit identification in drug discovery. Anal. Biochem., 2004, 332, 153-159.

[33] Andreotti, G. Monticelli, M.; Cubellis, M. V. Looking for protein stabilizing drugs with thermal shift assay. Drug Test. Anal., 2015, 7, 831-834.

[34] Li, C. J.; Liu, Y. X.; Wang, Q. M. Controllable and efficient oxidation of thioether by 2-iodoxybenzoic acid (IBX) in water: semisynthesis of sophocarpine. Tetrahedron Lett., 2014, 55, 950-953.

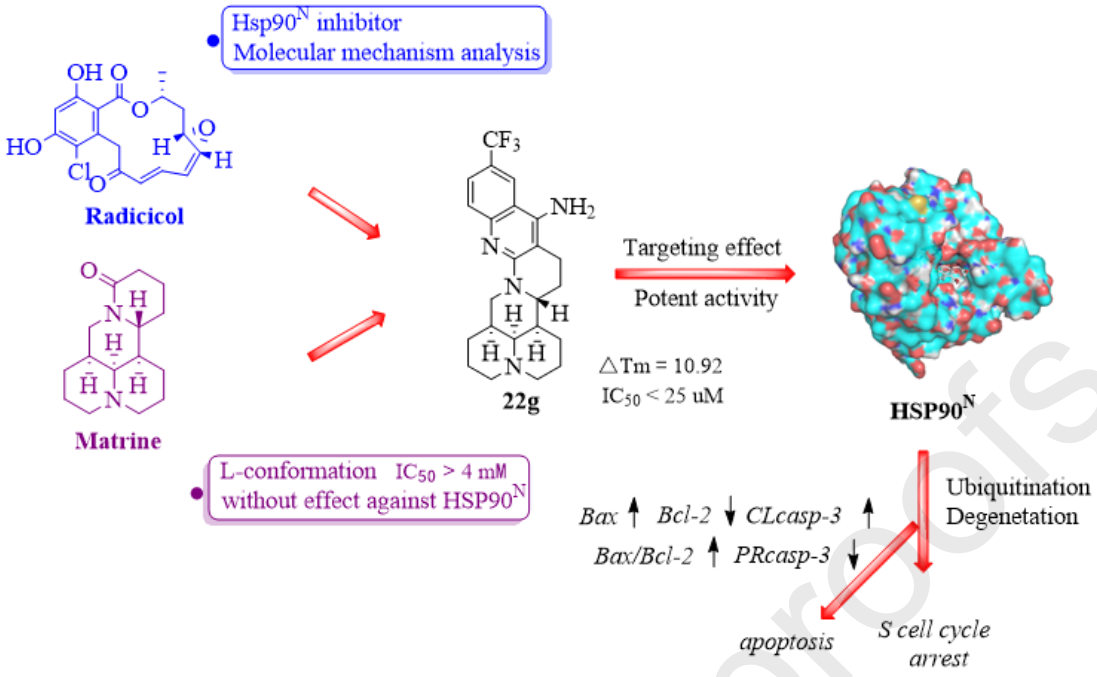

Conflict of interest

The authors declare no conflict of interest.